Experimental Verification of Theoretically Calculated Transition Barriers of the Reactions in a Gaseous Selective Oxidation of $CH_4-O_2-NO_2$

Kenji Tabata,* Yonghong Teng, Yoichi Yamaguchi,† Hiroaki Sakurai, and Eiji Suzuki

Research Institute of Innovative Technology for the Earth (RITE), Kizugawadai, Kizu-cho, 9−2, Soraku-gun, Kyoto, 619−0292 Japan

Received: July 27, 1999; In Final Form: January 11, 2000

The selective oxidation of methane with oxygen to C_1 oxygenates (methanol and formaldehyde) is an important process. However, the precise reaction mechanism in a gaseous chain reaction has not been clarified. Methane activation and the selectivity of C_1 oxygenates (CH_3OH, CH_2O) in a gaseous selective oxidation of $CH_4-O_2-NO_2$ have been examined under atmospheric pressure with both theoretical and experimental approaches. Theoretically calculated transition barrier of hydrogen abstraction from CH_4 of the reaction $CH_4 + NO_2 \rightarrow CH_3 + HNO_2$ was lower than that of the reaction with O_2, i.e., $CH_4 + O_2 \rightarrow CH_3 + O_2H$. This decrease of the transition barrier was experimentally verified by the linear enhancement of CH_4 conversion with NO_2 concentration in $CH_4-O_2-NO_2$. The experimental varied results of selectivity of C_1 oxygenates on various reaction conditions (NO_2 concentration, CH_4/O_2 ratio, space velocity) showed the appropriateness of the consideration on the selectivity with the calculated values of transition barriers and rate constants of the selected reaction routes from CH_3O to CH_3OH and CH_2O. After considering the transition barriers and rate constants of each elemental reaction route, we attained ca. 7% yield of C_1 oxygenates.

Introduction

The selective oxidation of methane with oxygen to C_1 oxygenates (methanol and formaldehyde) is an important process for the effective use of natural gas resources. In recent years, many researchers have studied the selective oxidation of natural gas with various types of catalysts. However, the products mostly comprise CO, CO_2, and H_2O with only trace formation of CH_3OH, CH_2O, and C_2H_6.[1−3] Accordingly, the metal-oxide catalysts that have been examined cause successive oxidation. The gas-phase reaction without catalysts seems to have the advantage of yielding C_1 oxygenates because the difficulty of the desorption stage from the surface of a catalyst could be liberated but the control of a chain reaction could be difficult. Formation of methanol and/or formaldehyde with methane and oxygen in a gaseous reaction has been reported.[2,4−14] Kinetic and thermodynamic models of these gaseous reactions have been discussed. The rate-determining step of the selective oxidation of methane is the first hydrogen abstraction from methane. Therefore, initiators and sensitizers have been examined in order to reduce the activation energy of the first hydrogen abstraction from methane.[14−16] The promotion effect of nitrogen oxides for methane selective oxidation in a gaseous reaction has been reported.[13,14,17−20] Bromly et al. prepared the kinetic models in $CH_4-O_2-NO_x$, based on the heats of formation and entropies.[14] The predictions of their kinetic models for the oxidation reactions in an atmospheric pressure were in good agreement with the experimental data over the entire range of conditions, though the main product of the reaction was CO, and the formation of C_1 oxygenates was not reported. Recently, Bañares et al.[21] reported a high yield of methanol and formaldehyde over V_2O_5/SiO_2 catalysts in the presence of NO. The highest yield of C_1 oxygenates (CH_3OH and CH_2O) reached 7% at atmospheric pressure. They suggested that the contribution of gas-phase reactions for the formation of C_1 oxygenates and the presence of NO must alter the equilibria in the gas-phase reactions.

Very recently, we proposed a reaction model for the conversion of methane to methanol and formaldehyde with CH_4-NO_x ($x = 1$ or 2) in the gas phase by means of theoretical calculations at the MP2 (frozen core) and CCSD(T) levels.[22] It was found that in both NO and NO_2, a nitrogen atom showed a higher activity for the cleavage of the C−H bond of methane than did an oxygen atom in NO_x. Furthermore, the activation energies were calculated as 62 kcal/mol for a nitrogen atom of NO and 37.6 kcal/mol for that of NO_2, indicating that NO_2 had higher activity for the hydrogen abstraction from methane than NO. Through the theoretical analysis of the CH_4-NO_2 reaction system in the previous paper, we suggested a possible reaction path leading to yield in both methanol and formaldehyde within all the barriers of less than 40 kcal/mol via CH_3O.[22] However, we did not consider the contribution from the coexistent oxygen to the reactions for the formation of C_1 oxygenates in $CH_4-O_2-NO_2$.[22]

In this study, we will examine exclusively the gaseous selective oxidation of methane with $CH_4-O_2-NO_2$ under atmospheric pressure. We will examine the effects of NO_2 on methane activation and the selectivities of methanol and formaldehyde with both experimental and theoretical approaches. Some of the experimental results were submitted as a letter.[23] We will study theoretically the role of coexistent oxygen on the reaction path leading to the selective formation of CH_3OH and CH_2O. We will examine on the applicability of our calculated transition barriers and rate constants of each elemental reaction route in order to consider the selectivities to CH_3OH and CH_2O under various reaction conditions, since the

* To whom correspondence should be addressed.
† Kansai Research Institute, Kyoto Research Park 17, Chudoji Minami-machi, Shimogyo-ku, Kyoto, 600-8813 Japan.

10.1021/jp9926239 CCC: $19.00
Published on Web 02/26/2000

detailed mechanisms of the selectivities to CH_3OH and CH_2O for the gaseous chain reactions in $CH_4-O_2-NO_2$ have not been made clear.

Experimental Section

The reaction test was carried out using a single-pass flow reactor made of a quartz tube with an inside diameter of 7.0 mm and a heated length of 200 mm. The total flow rate was 120 $cm^3\ min^{-1}$. The standard gas composition (CH_4: 55.6%, O_2: 27.7%, NO_2: 0.5%, He: 16.2%) was controlled with a mass flow controller. The concentration of NO_2 ranged from 0.125% to 1.0%; however, the ratio of CH_4 to O_2 was 2.0, unless otherwise indicated. The products were analyzed with two on-line gas chromatographs serially connected. A thermal conductivity detector (Molecular Sieve 5A) and a flame ion detector (Porapack Q), using helium as a carrier gas, were used. The carbon balance before and after the reaction exceeded 95%. Measurements were carried out after 30 min of reacting at each experimental condition, and all experimental data were taken at least three times to check the reproducibility.

Method of Calculation. All of the calculations were carried out with the *Gaussian 94* ab initio program package.[24] The geometrical optimization for all of the present molecules was performed with the MP2 (frozen core) level of theory and 6-311++G(2d, p) basis set. On the basis set of the optimized geometries, the single point calculations of the energies were calculated at the CCSD(T)/6-311++G(2d, p) level with the zero-point energy corrections of the MP2 level. Thermal rate constants for all of the present elementary reactions at 800 K and 1 atm were also estimated using the calculated results of MP2 and CCSD(T) levels of theory. A Silicon Graphics Origin 2000 R10000 workstation was used for calculations in this study.

Results

Methane Activation. The rate-determining step of the selective oxidation of methane is the first abstraction of hydrogen atom. The high barrier value as 55.2 kcal/mol has been calculated theoretically for the $O_2 + CH_4 \rightarrow CH_3 + O_2H$ reaction.[22] We calculated the methane activation barriers of the optimized transition structures with NO_2 as follows:

$$NO_2 + CH_4 \rightarrow [TS1] \rightarrow HNO_2 + CH_3 \qquad (1)$$

$$NO_2 + CH_4 \rightarrow [TS2] \rightarrow \textit{trans}\text{-}HONO + CH_3 \qquad (2)$$

where the total energy of $CH_4 + NO_2$ is taken as a standard. The transition barrier for eq 1 is calculated as 37.6 kcal/mol. Equation 2 has a barrier of 45.8 kcal/mol. These barriers for the reactions in eqs 1 and 2 are significantly lower by 9−18 kcal/mol than the above-mentioned $O_2 + CH_4 \rightarrow O_2H + CH_3$ reaction, which indicates a higher activity of CH_4 in the presence of NO_2 for the reaction of hydrogen abstraction from methane in comparison with O_2.

Figure 1 shows the emergent region of methane conversion as a function of reaction temperature. The conversion without NO_2, i.e., $CH_4 + O_2$ shows a quite low activity even at 966 K. The addition of a small quantity of NO_2 in the reaction gas enhances the conversion greatly. The reactivity increases with the concentration of NO_2 to 0.75% in $CH_4-O_2-NO_2$ mixed gas. The calculated transition barrier in the presence of NO_2 from this experiment is 45.7 kcal/mol at the level of 10% CH_4 conversion. This value is close to the reported experimentally obtained value (49.7 kcal/mol).[20] This increase of reactivity seems to be led by the decrease of the transition barrier of hydrogen atom abstraction from methane for the reaction path of CH_4-NO_2 instead of CH_4-O_2 as we expected from the theoretical calculation. Therefore, the reaction of hydrogen atom abstraction from methane mainly progresses on the reaction route of CH_4-NO_2.

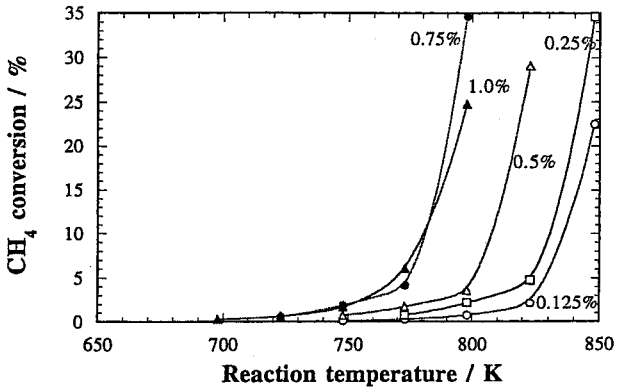

Figure 1. CH_4 conversion variation at different NO_2 concentration as a function of reaction temperature. Reaction gas: CH_4 (55.6%) + O_2 (27.7%) + NO_2 in He (balance). Flow rate: 120 mL/min.

Methoxide Formation. We calculated the formation route of CH_3O, which is an important intermediate because only CH_3O can lead to yield CH_3OH and CH_2O.[22] The coupling CH_3 with NO_2 directly produces CH_3NO_2 and *trans*-CH_3ONO. Each stabilization energy was 57.0 and 55.7 kcal/mol, respectively. The thermal decomposition of *trans*-CH_3ONO into CH_3O and NO via [TS3] was calculated.[22]

$$\textit{trans}\text{-}CH_3ONO \rightarrow [TS3] \rightarrow CH_3O + NO \qquad (3)$$

The transition barrier of this decomposition reaction was calculated as 38.4 kcal/mol.

We did not consider the contribution of oxygen to CH_3O formation in the previous paper.[22] However, the methyl radical is assumed to react easily with oxygen. We calculated the transition barriers of the following four reaction routes of CH_3O formation. The calculation method is the same as with our previous paper.[22]

$$O_2 + CH_3 \rightarrow [TS4] \rightarrow CH_3OO \qquad (4)$$

$$CH_3OO + CH_4 \rightarrow [TS5] \rightarrow CH_3OOH + CH_3 \qquad (5)$$

$$CH_3OOH \rightarrow [TS6] \rightarrow CH_3O + OH \qquad (6)$$

$$CH_3OO + NO \rightarrow [TS7] \rightarrow CH_3O + NO_2 \qquad (7)$$

Each calculated transition barrier is shown in Figure 2. Here the state of the separated reactants is taken as a standard. The optimized geometries of transition states [TS4] and [TS7] with the C_S structures and [TS5] and [TS6] with the C_1 structures are illustrated in Figure 3. The highest transition barrier in eqs 4−7 is 37.8 kcal/mol, and it is calculated as that of [TS6] in eq 6. Since the value of the transition barriers of [TS6] and those of [TS1] and [TS2] are almost the same, all of the reactions in eqs 4−6 are assumed to be possible to make progress. If the concentration of NO in the reactant gas is sufficient, CH_3OO will react with NO to form CH_3O through [TS7] in eq 7. This route is energetically favorable in comparison with the routes

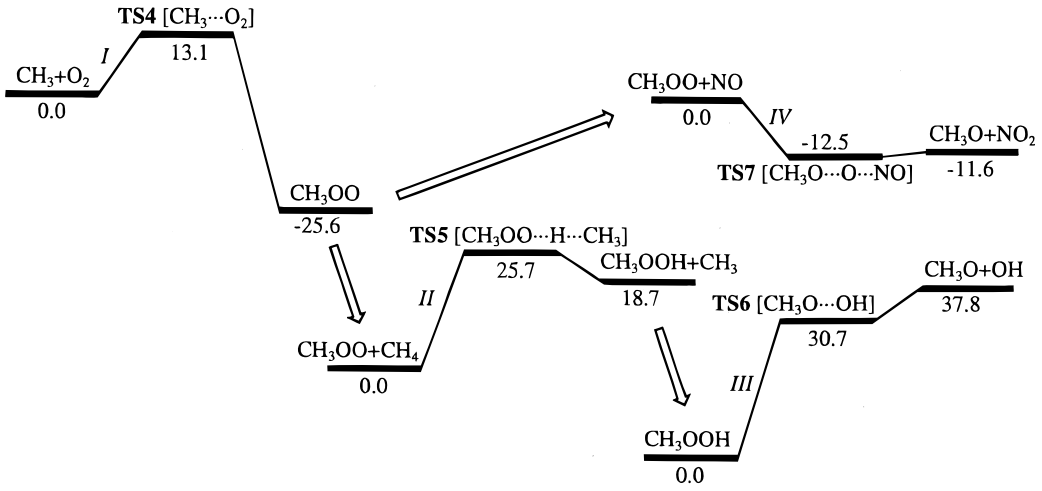

Figure 2. Potential energy diagram for the formation of CH_3O through CH_3OO. The total energies for the separated reactants $O_2 + CH_4$ (I), $CH_3OO + CH_4$ (II), CH_3OOH (III), and $CH_3OO + NO$ (IV) are −189.7868, −230.1974, 190.4562, and −319.4922 hartrees, respectively. Relative energies are given in kcal/mol.

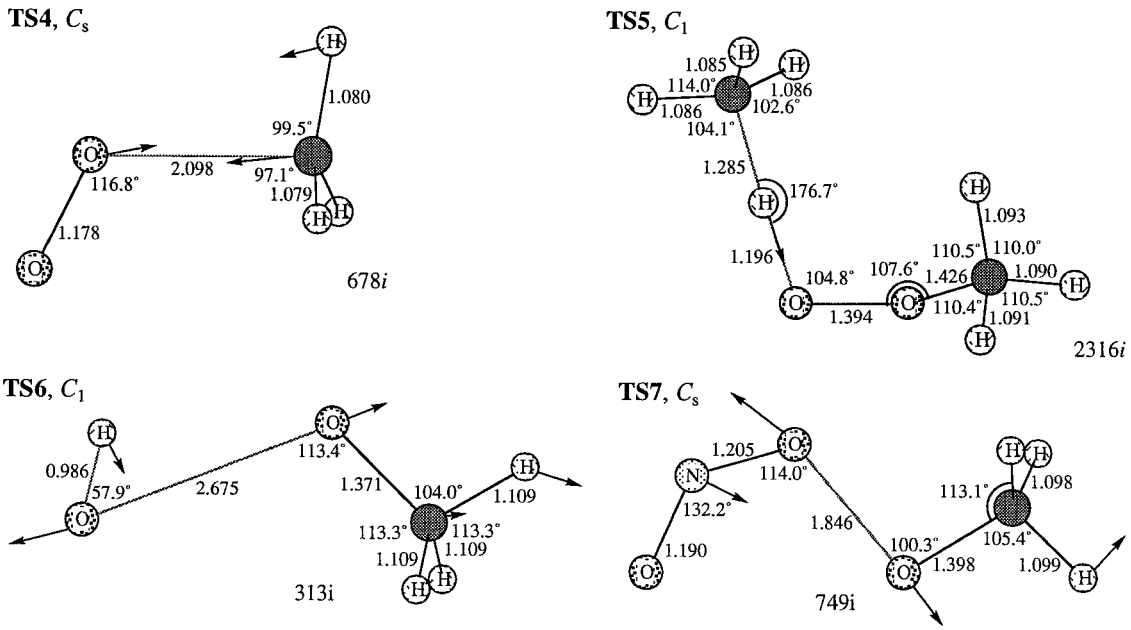

Figure 3. Optimized geometries for TS4 of the $CH_3 + O_2$ reaction, TS5 of the $CH_3OO + CH_4$ reaction, TS6 of the decomposition of CH_3OOH, and TS7 of the $CH_3OO + NO$ reaction. All bond lengths and bond angles are given in Å and degrees, respectively. Imaginary frequency modes for the forward reactions are given in cm^{-1}.

TABLE 1: Calculated Rate Constants, *k*, and Activation Energies, E_A, at 800 K[a]

reaction	*k*	E_A (kcal/mol)
$CH_4 + NO_2 \rightarrow CH_3 + H-NO_2$[b]	5.4×10^{-20}	37.6
$CH_4 + NO_2 \rightarrow CH_3 +$ *trans*-HONO[b]	3.3×10^{-22}	45.8
trans-$CH_3ONO \rightarrow CH_3O + NO$[b]	2.5×10^{-5}	35.6
$CH_3 + O_2 \rightarrow CH_3OO$	1.3×10^{-15} (2.0×10^{-12})	14.8 (0.0)
$CH_3OO + CH_4 \rightarrow CH_3OOH + CH_3$	3.3×10^{-19} (1.3×10^{-18})	29.9 (21.5)
$CH_3OOH \rightarrow CH_3O + OH$	1.5×10^{6} (7.2×10^{3})	33.0 (43.0)
$CH_3OO + NO \rightarrow CH_3O + NO_2$	1.5×10^{-10} (5.3×10^{-12})	−9.7 (−0.4)
$CH_3O + CH_4 \rightarrow CH_3OH + CH_3$[b]	1.8×10^{-15} (9.9×10^{-16})	16.9 (11.0)
$CH_3O \rightarrow CH_2O + H$[b]	2.2×10^{6} (6.4×10^{5})	27.5 (30.0)
$CH_3O + O_2 \rightarrow CH_2O + HO_2$	1.7×10^{-17} (1.7×10^{-14})	21.7 (2.1)
$CH_3O + NO_2 \rightarrow CH_2O + H-NO_2$[b]	1.1×10^{-15}	6.7
$CH_3O + NO \rightarrow CH_2O + HNO$[b]	3.1×10^{-14} (2.6×10^{-12})	5.6 (−0.4)

[a] Values in parentheses represent the experimental data taken from refs 4 and 14. Rate constants are in s^{-1} and cm^3 $molecule^{-1}$ s^{-1} for unimolecular and bimolecular reactions, respectively. Activation energies are in kcal/mol. [b] From ref 22.

through eqs 5 and 6. The calculated rate constants and activation energies at 800 K are listed in Table 1. The data were calculated using the conventional transition-state theory and using the calculated results of MP2 and CCSD(T) levels of theory. The reported values of activation energies and rate constants are listed in Table 1 also for comparison.

Reaction Routes to CH_3OH and CH_2O. The elementary reactions for yielding CH_3OH and CH_2O from CH_3O are shown

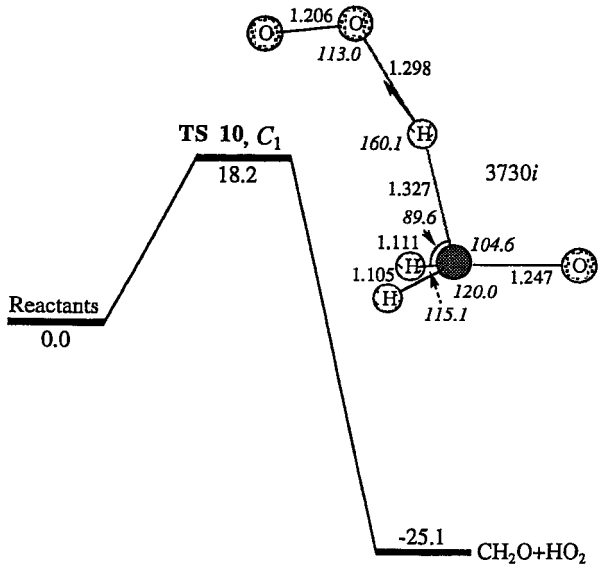

Figure 4. Potential energy diagram for the $CH_3O + O_2$ reaction with the optimized geometry for TS10. The total energy for the separated reactants is −264.8679 hartrees. Relative energies are given in kcal/mol.

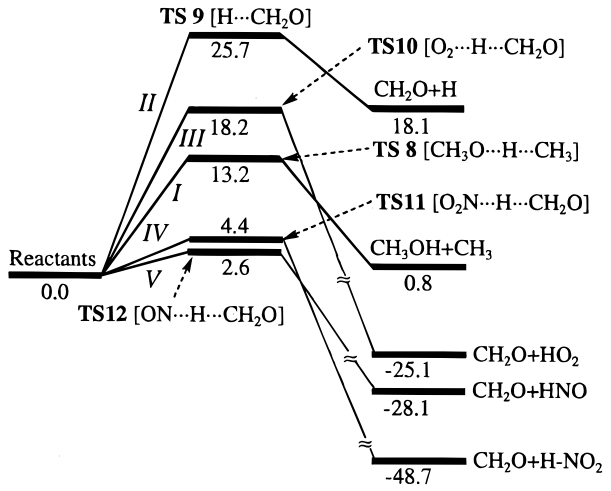

Figure 5. Potential energy diagram for the formation of C_1 oxygenates. The total energies for the separated reactants $CH_3O + CH_4$ (I), CH_3O (II), CH_3O+O_2 (III), $CH_3O + NO_2$ (IV), and $CH_3O + NO$ (V) are −155.1623, −114.7925, −264.8679, −319.5106, and −244.4570 hartrees, respectively. Relative energies are given in kcal/mol.

as follows:

$$CH_3O + CH_4 \rightarrow [TS8] \rightarrow CH_3OH + CH_3 \quad (8)$$

$$CH_3O \rightarrow [TS9] \rightarrow CH_2O + H \quad (9)$$

$$CH_3O + O_2 \rightarrow [TS10] \rightarrow CH_2O + HO_2 \quad (10)$$

$$CH_3O + NO_2 \rightarrow [TS11] \rightarrow CH_2O + H{-}NO_2 \quad (11)$$

$$CH_3O + NO \rightarrow [TS12] \rightarrow CH_2O + H{-}NO \quad (12)$$

The transition barriers except for [TS10] were reported in the previous paper,[22] and we calculated [TS10] in order to examine the contribution to CH_2O formation from coexistent O_2 with the same calculation procedures. The calculated transition barrier and the optimized geometries of transition states are shown in Figure 4. The complete potential energy diagram for eqs 8−12 is illustrated in Figure 5, where the total energy of each separated reactant is taken as a standard. The highest transition barrier is 25.7 kcal/mol for the thermal decomposition of CH_3O in eq 9. All of the transition barriers in eqs 8−12 are lower than that of hydrogen atom abstraction in eq 1. Therefore, all of the reactions of eqs 8−12 are energetically possible to proceed. The calculated rate constants of these reactions are listed in Table 1 also.

Regarding the selectivities of CH_3OH and CH_2O, one of the important points is that CH_3OH is produced only from reaction 8. The second important point is that the transition barriers of CH_2O formation from CH_3O and NO_2 or NO (assumed to be produced during the reaction in the reactor) in eqs 11 and 12 are lower than [TS8] for the CH_3OH formation.

We show our suggested reaction routes up to the formation of CH_3OH and CH_2O (Figure 6). The largest value of the calculated transition barrier is 45.8 kcal/mol, which is given from the reaction for the first hydrogen abstraction from CH_4.

Decomposition Route from CH_3OH and CH_2O. We addressed the reaction routes for the formation of CH_3OH and CH_2O, but the reaction routes for the decomposition of CH_3OH and CH_2O are assumed to affect strongly the selectivities of those. The decomposition routes of CH_3OH and CH_2O have been suggested widely.[4,5,14] In the suggested routes, we focused on the route with OH species:

$$CH_3OH + OH \rightarrow CH_2OH + H_2O \quad (13)$$

$$CH_2OH + O_2 \rightarrow CH_2O + HO_2 \quad (14)$$

$$CH_2O + OH \rightarrow CHO + H_2O \quad (15)$$

$$CHO + O_2 \rightarrow CO + HO_2 \quad (16)$$

The transition barrier in eq 13 was reported as 1.4 kcal/mol,[4] and the others in eqs 14−16 were less than this value. Therefore, if OH species are sufficient in the gaseous phase, the reaction for the decomposition of CH_3OH and CH_2O proceeds easily. The decomposition routes of CH_3OH and CH_2O with coexistent NO_2 also should be considered:

$$CH_3OH + NO_2 \rightarrow CH_2OH + HONO \quad (17)$$

$$CH_2O + NO_2 \rightarrow CHO + HONO \quad (18)$$

The transition barriers of these reactions are reported as 21.4 and 16.1 kcal/mol, respectively.[14] We calculated also the transition barriers of the following reactions with coexistent NO_2 as 28.3 and 21.4 kcal/mol, respectively:

$$CH_3OH + NO_2 \rightarrow CH_2OH + HNO_2 \quad (19)$$

$$CH_2O + NO_2 \rightarrow CHO + HNO_2 \quad (20)$$

Experimental Results of the Selectivities of CH_3OH and CH_2O. *NO_2 Concentration.* The concentration of NO_2 in a reactant gas should affect not only the conversion of CH_4 but also the selectivities of CH_3OH and CH_2O. Figure 7 shows the selectivities of the products as a function of NO_2 concentration at the same 10% methane conversion. The selectivity of CH_3OH is higher than that of CH_2O in the range of 0.25−1.0% NO_2 concentration. This is the first report that the selectivity

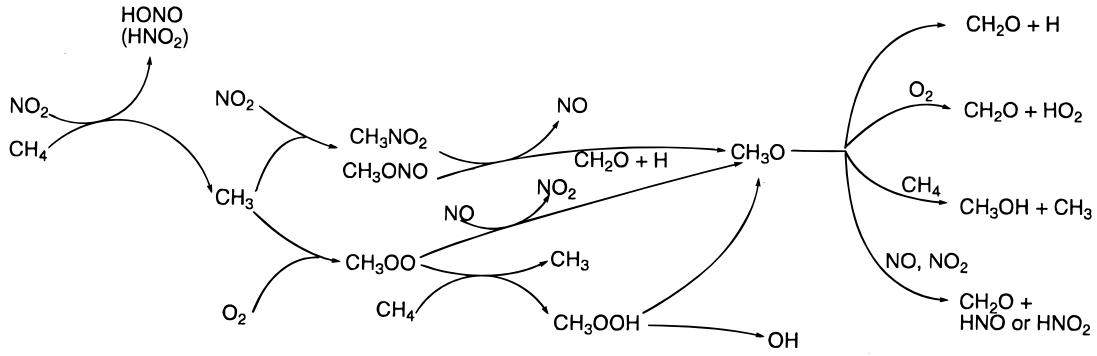

Figure 6. Suggested reaction pathways for the formation of CH_3OH and CH_2O in $CH_4-O_2-NO_2$.

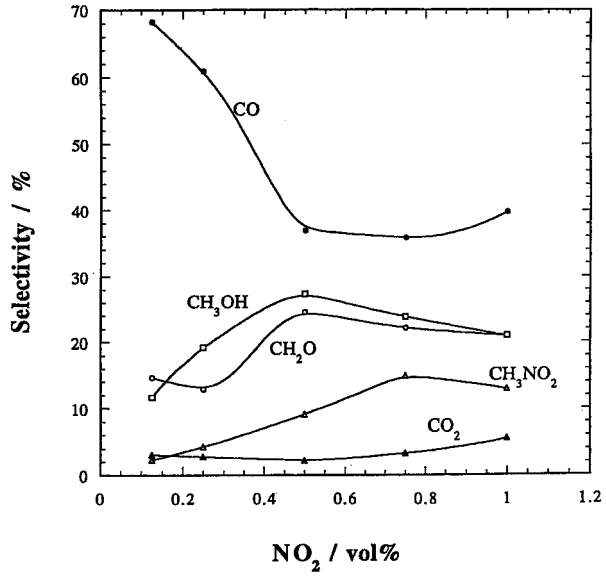

Figure 7. Selectivity variation as a function of NO_2 concentration at 10% CH_4 conversion with CH_4 (55.6%) + O_2 (27.7%) + NO_2 in He (balance).

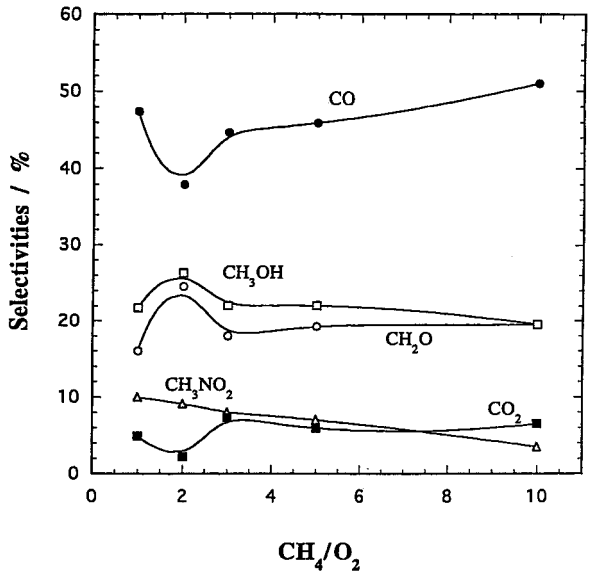

Figure 8. Selectivity variation at the level of 10% CH_4 conversion as a function of CH_4/O_2 ratio. The percentages of CH_4 and O_2 in the feed gas were changed so as to change the ratio of CH_4/O_2 from 1 to 10. The percentages of NO_2 and He were fixed at 0.5% and 16.2%, respectively except for the case at $CH_4/O_2 = 1$. The percentages of NO_2 and He were 0.5% and 44.0%, respectively, at $CH_4/O_2 = 1$.

of CH_3OH exceeds that of CH_2O in the gaseous selective oxidation of $CH_4-O_2-NO_2$ under atmospheric pressure. Both selectivities in Figure 7 increased from 0.25% to 0.5%, then decreased slightly to 1.0%. The selectivity of CO decreased until NO_2 reached 0.75%, then increased again. The ratio of CH_2O to CH_3OH increased gradually in the region of 0.25−1.0% NO_2 concentration.

CH_4/O_2 Ratio. The ratio of coexistent methane to oxygen in the reactant gas is theoretically assured to affect the selective yields of CH_3OH and CH_2O (Figure 5). We experimentally studied the effects of the CH_4/O_2 ratio on each selectivity of CH_3OH and CH_2O. Figure 8 shows each selectivity of products at the 10% conversion of CH_4 as a function of the ratio of CH_4:O_2 in $CH_4-O_2-NO_2$ reactant gas. The conversion of CH_4 as a function of reaction temperature on each ratio from 1 to 10 is shown in Figure 9. The selectivity of CH_3OH is higher than that of CH_2O in the range of 1 to 10. One feature of the results in Figure 8 is the highest yield of both CH_3OH and CH_2O at $CH_4/O_2 = 2$.

Space Velocity (SV). We studied the effects of space velocity (SV) on the selectivities. The SV was calculated by dividing the gas flow volume per 1 h at 298 K and 1 bar by the volume of the vacant heated zone of the reactor. Figure 10 shows the variation of each selectivity with SV at 10% methane conversion. CH_2O increases with SV but CO decreases. These changes of both CH_2O and CO agree well with the obtained results by Irusta et al.[18] This means that CO is a secondary product following the formation of CH_2O. The selectivities of CH_3OH and CO_2 are less affected by the SV variation in comparison with CH_2O and CO. All of these data were detected close to 800 K, in other words, the difference of each detected reaction temperature at the 10% methane conversion is less than 10 K (Figure 11).

Discussion

It has been known for more than 70 years that the oxidation of CH_4 with O_2 can be accelerated by the addition of NO.[25] Recently, Otsuka et al. examined the partial oxidations of CH_4, C_2H_6, C_3H_8, and *iso*-C_4H_{10} with O_2 by addition of NO in the gas phase.[20] Regarding the contribution of NO_x to the activation of methane, they suggested that NO_2 would work as an initiator or oxidant in the oxidations because the reaction between NO and alkane did not take place in the absence of O_2. Thus they speculated that some NO_2-containing hydrocarbons could be the reaction intermediate for the formation of oxygenates. They examined the decomposition reactions of 1-$C_3H_7NO_2$, 2-$C_3H_7NO_2$, and *tert*-C_4H_9ONO in the flow of O_2 or a mixture of NO and O_2 and detected the formation of HCHO, CO, CO_2, and CH_3NO_2 from only the decomposition of *tert*-C_4H_9ONO. They suggested that alkyl nitrite could be the intermediate for the formation of oxygenates. From these experimental results, they

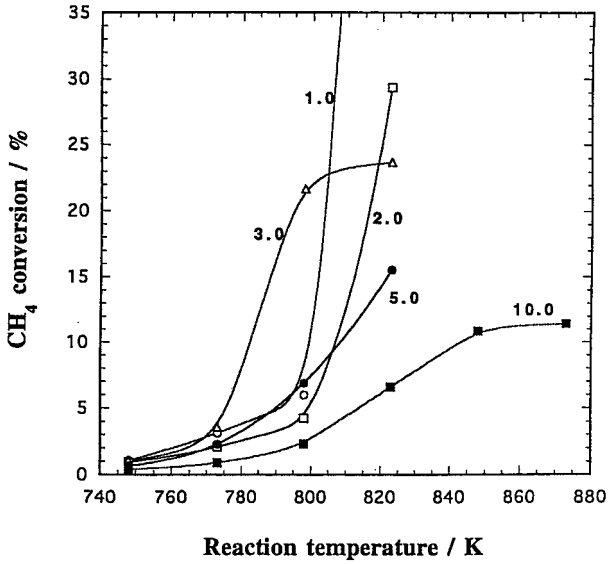

Figure 9. CH_4 conversion under different CH_4/O_2 ratios as a function of reaction temperature. The percentages of CH_4 and O_2 in the feed gas were changed so as to change the ratio of CH_4/O_2 from 1 to 10. The percentages of NO_2 and He were fixed at 0.5% and 16.2%, respectively, except for the case at $CH_4/O_2 = 1$. The percentages of NO_2 and He were 0.5% and 44.0%, respectively, at $CH_4/O_2 = 1$.

suggested a reaction scheme. Their suggested scheme is listed as follows:

$$NO + 1/2\ O_2 \rightarrow NO_2 \quad (21)$$

$$CH_4 + NO_2 \rightarrow CH_3 + HNO_2 \quad (22)$$

$$CH_3 + NO_2 \rightarrow CH_3ONO \quad (23)$$

$$CH_3 + NO_2 \rightarrow CH_3NO_2 \quad (23')$$

$$CH_3ONO \rightarrow CH_3O + NO \quad (24)$$

$$CH_3O \rightarrow CH_2O + H \quad (25)$$

$$CH_3 \xrightarrow{O_2,\ NO_2} HCHO,\ CO,\ CO_2 \quad (26)$$

The details in eq 26 were not clear. Furthermore, the reaction route to the formation of CH_3OH was not discussed. Especially, the details of the transition barriers and rate constants for addressing the selectivities of CH_3OH and CH_2O have not been made clear yet.

We have tried to connect the theoretically calculated transition barriers and rate constants of elemental reaction routes for the formation of CH_3OH and CH_2O and to the experimentally observed selectivities of those. The effects of NO_2 concentration, the ratio of CH_4/O_2, and SV on the selective yields of CH_3OH and CH_2O were experimentally examined. We addressed the theoretically obtained transition barriers and rate constants and the variations of observed selectivities of CH_3OH and CH_2O under several reaction conditions at the same time. In Table 1, the calculated values of [TS4] and [TS8] are much different from the reported experimental values.[4,14] We assumed that the main reason of for this difference came from the reactions between a doublet state (CH_3, CH_3O) and a triplet state (O_2) species, which caused a large spin contamination in the results at the level of our calculations. Regarding the effects of NO_2 concentration on the selectivities of CH_3OH and CH_2O (Figure 7), both selectivities increased in the range from 0.25% to 0.5%.

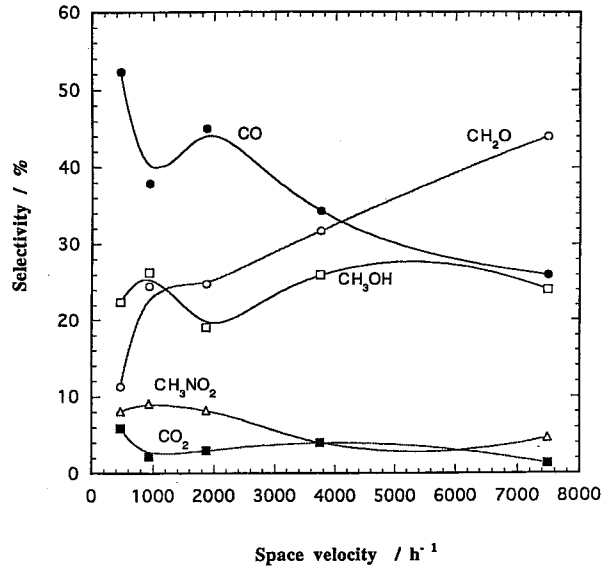

Figure 10. Selectivity variation at the level of 10% CH_4 conversion as a function of space velocity (SV) with CH_4 (55.6%) + O_2 (27.7%) + NO_2 (0.5%) in He (balance).

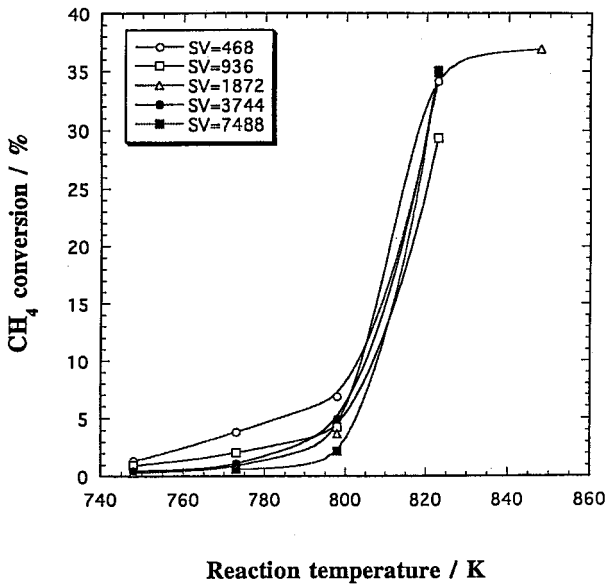

Figure 11. CH_4 conversion at different space velocity (SV) as a function of reaction temperature with CH_4 (55.6%) + O_2 (27.7%) + NO_2 (0.5%) in He (balance).

The selectivity of CO decreased rapidly in the same range. Therefore, we considered that the increase of the selectivities of CH_3OH and CH_2O resulted from the decline of decomposition reactions of CH_3OH and CH_2O with OH in eqs 13−16. The reaction route for the formation of OH is known from eq 6. The transition barrier of [TS6] is 37.8 kcal/mol (Figure 2), and this value is much higher than that of [TS7] for the formation of CH_3O. Additionally, there is no transition barrier for the reverse reaction from CH_3O to CH_3OOH. Therefore, the reaction route for the decomposition of CH_3OO in eq 7 is favorable to form CH_3O. Furthermore, since the rate constant of eq 7 is larger than that of eq 5, CH_3OO is assumed to react with NO. Therefore, the concentration of OH in the gas phase of $CH_4-O_2-NO_2$ could be low in comparison with that in the gas phase of CH_4-O_2. This low concentration of OH could bring the decline of decomposition reaction, then the selectivities of CH_3OH and CH_2O increased in the range of 0.1−0.5% NO_2 concentration. Furthermore, we must point out the effect of

reaction temperature. We compared the product selectivities at the level of 10% CH_4 conversion. We therefore compared the data at different temperatures in order to assess the effect of NO_2 concentration. The reaction temperature at the level of CH_4 conversion decreased by the addition of NO_2 (Figure 1). This decrease may suppress the subsequential oxidation to CO. Additionally, since higher NO_2 concentration over 0.5% brings a slight decrease of both selectivities of CH_3OH and CH_2O, the decomposition reaction of CH_3OH and CH_2O with NO_2 in eqs 17−20 could affect their selectivities.

Regarding the CH_4/O_2 ratio, we expected an increase of selectivity of CH_3OH and a decrease of selectivity of CH_2O from eqs 8 and 10 as the ratio increased. The variations on the selectivities of CH_3OH and CH_2O are small except for $CH_4/O_2 = 2$ during the region of our experiments (Figure 8). Furthermore, another feature of the experimental result is the parallel movement of the selectivities of CH_3OH and CH_2O in that region. The selectivities of CO and CO_2 decrease at $CH_4/O_2 = 2$ and that of CO increases slightly after the ratio exceeds 2. Therefore, we considered that CH_3OH produced through eq 8 could be decomposed subsequently to CO through eqs 13−16. The increase of the reaction temperatures at the 10% CH_4 conversion in Figure 9 is assumed to enhance the subsequential oxidation to CO. $CH_4/O_2 = 2$ is optimum for the formation of CH_3OH and CH_2O.

Regarding the variation with SV, the selectivities of CH_2O and CO seem to move in conjunction (Figure 10). The decrease of CO and the increase of CH_2O in the selectivities are assumed to be the result of the retardation of the subsequent oxidation from CH_2O to CO. The less variation of CH_3OH selectivity with SV shows that CH_3OH is more stable. The transition barriers of the decomposition route in eqs 13 and 15 are 1.4 and 0.2 kcal/mol, respectively.[4] The small difference between the transition barriers is assumed to lead to the large difference of selectivities of CH_3OH and CH_2O under a higher SV region. We obtained ca. 7% yield of C_1 oxygenates at SV = 7500 h^{-1} (Figure 10).

Conclusion

The anticipation of the selectivity of reaction products in a gaseous chain reaction is still difficult, and the precise reaction mechanisms have not been cleared. We examined several possible contributing reactions for the production of CH_3OH and CH_2O in gaseous selective oxidation with $CH_4-O_2-NO_2$ with both theoretical and experimental approaches. We theoretically calculated several transition barriers and rate constants of our suggested reaction routes. We can appropriately explain the experimentally detected selectivities of C_1 oxygenates by using the calculated transition barriers and rate constants of the reaction routes.

Acknowledgment. This study was financially supported by the New Energy and Industrial Technology Development Organization (NEDO, Japan). K.T. acknowledges Prof. J. L. G. Fierro and his colleagues for their kind discussions.

References and Notes

(1) Taylor, S. H.; Hargreaves, J. S.; Hutchings, G. J.; Joyner, W. J. *Methane and Alkane Conversion Chemistry*; Plenum: New York, 1995; p 339.
(2) Pitchai, R.; Klier, K. *Catal. Rev. −Sci. Eng.* **1986**, *28*, 13.
(3) Pak, S.; Rosynek, M. P.; Lunsford, J. H. *J. Phys. Chem.* **1994**, *98*, 11786.
(4) Arutyunov, V. S.; Basevich, V. Y.; Vedeneev, V. I. *Russ. Chem. Rev.* **1996**, *65*, 197.
(5) Mackie, J. C. *Catal. Rev. −Sci. Eng.* **1991**, *33*, 169.
(6) Foster, N. R. *Appl. Catal.* **1985**, *19*, 1.
(7) Gesser, H. D.; Hunter, N. R.; Prakash, C. B. *Chem. Rev.* **1985**, *85*, 235.
(8) Burch, R.; G. D. Squire, G. D.; Tsang, S. C. *J. Chem. Soc., Faraday Trans. 1.* **1989**, *85*, 3561.
(9) Baldwin, R. R.; Hopkins, D. E.; Norris, A. C.; Walker, R. W. *Combust. Flame.* **1970**, *15*, 33.
(10) Thomas, D. J.; Willi, R.; Baiker, A. *Ind. Eng. Chem. Res.* **1992**, *31*, 2272.
(11) Krylov, O. V. *Catal. Today* **1993**, *18*, 209.
(12) Feng, W.; Knopf, F. C.; Dooley, K. M. *Energy Fuels* **1994**, *8*, 815.
(13) Amano, T.; Dryer, F. L. *Twenty-Seventh Symposium (International) on Combustion*; The Combustion Institute: Pittsburgh, 1998; p 397.
(14) Bromly, J. H.; Barnes, F. J.; Muris, X. Y.; Haynes, B. S. *Combust. Sci. Technol.* **1996**, *115*, 259.
(15) Wharren, B. K. *Catal. Today* **1992**, *13*, 311.
(16) Burch, R.; Squire, G. D.; Tsang, S. C. *Appl. Catal.* **1989**, *46*, 69.
(17) Smith, D. F.; Milner, R. T. *Ind. Eng. Chem.* **1931**, *23*, 357.
(18) Irusta, S.; Lombardo, E. A.; Miro, E. E. *Catal. Lett.* **1994**, *29*, 339.
(19) Han, L. B.; Tsubota, S.; Haruta, M. *Chem. Lett.* **1995**, 931.
(20) Otsuka, K.; Takahashi, R.; Amakawa, K.; Yamanaka, I. *Catal. Today* **1998**, *45*, 23. Otsuka, K.; Takahashi, R.; Amakawa, K.; Yamanaka, I. *Proceed. JECAT* **1997**, 41.
(21) Bañares, M. A.; Cardoso, J. H.; Hutchings, G. J.; Bueno J. M. C.; Fierro, V. L. G. *Catal.Lett.* **1998**, *56*, 149.
(22) Yamaguchi, Y.; Teng, Y.; Shimomura, S.; Tabata, K.; Suzuki, E. *J. Phys. Chem.*, in press.
(23) Teng, Y.; Ouyang F.; Dai, L.; Karasuda T.; Sakurai H.; Tabata K.; Suzuki E. *Chem. Lett.* **1999**, 991.
(24) Frisch, M. J.; Trucks, G. W.; Schlegel, H. B.; Gill, P. M. W.; Johnson, B. G.; Robb, M. A.; Cheeseman, J. R.; Keith, T. A.; Patterson, G. A.; Montgomery, J. M.; Raghavachari, K.; Al-Laham, M. A.; Zakrzewski, V. G.; Ortiz, J. V.; Foresman, J. B.; Cioslowski, J.; Stefanov, B. B.; Nanayakkara, A.; Challacombe, M.; Peng, C. Y.; Ayala, P. Y.; Chen, W.; Wong, M. W.; Andres, J. L.; Replogle, E. S.; Gomperts, R.; Martin, R. L.; Fox, D. J.; Binkley, J. S.; Defrees, D. J.; Baker, J.; Stewart, J. J. P.; Head-Gordon, M.; Gonzalez, C.; Pople, J. A. *Gaussian 94*, Gaussian Inc., Pittsburgh, PA, 1995.
(25) Layng, T. E.; Soukop, R. *Ind. Eng. Chem.* **1928**, *20*, 1052.